Author(s): Svärd, Laura; Putkonen, Matti; Kenttä, Eija; Sajavaara, Timo; Krahl, Fabian; Karppinen, Maarit; Kerckhove, Kevin Van de; Detavernier, Christophe; Simell, Pekka

Title: Low-temperature Molecular Layer Deposition Using Monofunctional Aromatic Precursors and Ozone-based Ring Opening Reactions

Year: 2017

Version:

Please cite the original version:

Svärd, L., Putkonen, M., Kenttä, E., Sajavaara, T., Krahl, F., Karppinen, M., Kerckhove, K. V. D., Detavernier, C., & Simell, P. (2017). Low-temperature Molecular Layer Deposition Using Monofunctional Aromatic Precursors and Ozone-based Ring Opening Reactions. Langmuir, 33(38), 9657-9665. https://doi.org/10.1021/acs.langmuir.7b02456

LANGMUIR

Article

Low-temperature Molecular Layer Deposition Using Monofunctional Aromatic Precursors and Ozone-based Ring Opening Reactions

Laura Kaisa Kristiina Svärd, Matti Putkonen, Eija Kenttä, Timo Sajavaara, Fabian Krahl, Maarit Karppinen, Kevin Van de Kerckhove, Christophe Detavernier, and Pekka Simell

Langmuir, **Just Accepted Manuscript** • DOI: 10.1021/acs.langmuir.7b02456 • Publication Date (Web): 24 Aug 2017

ACS Publications

Langmuir is published by the American Chemical Society. 1155 Sixteenth Street N.W., Washington, DC 20036

Low-temperature Molecular Layer Deposition Using Monofunctional Aromatic Precursors and Ozone-based Ring Opening Reactions

Laura Svärd[1], Matti Putkonen[1], Eija Kenttä[1], Timo Sajavaara[2], Fabian Krahl[3], Maarit Karppinen[3], Kevin Van de Kerckhove[4], Christophe Detavernier[4], Pekka Simell[1]*

1 VTT Technical Research Centre of Finland, P.O. Box 1000, 02044 VTT, Espoo, Finland

2 University of Jyvaskyla, Department of Physics, P.O. Box 35, FI-40014, Jyvaskyla, Finland

3 Aalto University, Department of Chemistry, School of Chemical Technology, P.O. Box 16100 FI-00076 Espoo, Finland

4 Ghent University, Department of Solid State Sciences, Krijgslaan 281/S1, Gent B-9000, Belgium

KEYWORDS: ALD, MLD, monofunctional aromatics, low-temperature, hybrid organic-inorganic, ring opening reaction, mechanism

ABSTRACT

Molecular Layer Deposition (MLD) is an increasingly used deposition technique for producing thin coatings consisting of purely organic or hybrid inorganic-organic materials. When organic materials are prepared, low deposition temperatures are often required to avoid decomposition, thus causing problems with low vapour pressure precursors. Monofunctional compounds have higher vapour pressures than traditional bi- or tri-functional MLD precursors, but do not offer the required functional groups for continuing the MLD growth in subsequent deposition cycles. In this study, we have used high vapour pressure monofunctional aromatic precursors in combination with ozone-triggered ring opening reactions to achieve sustained sequential growth. MLD depositions were carried out by using three different aromatic precursors in an ABC sequence, namely with TMA+phenol+O_3, TMA+3-(trifluoromethyl)phenol+O_3 and TMA+2-fluoro-4-(trifluoromethyl)benzaldehyde+O_3. Furthermore, the effect of hydrogen peroxide as a fourth step was evaluated for all studied processes resulting in a four-precursor ABCD sequence. According to the characterisation results by ellipsometry, infrared spectroscopy and X-ray reflectivity, self-limiting MLD processes could be obtained between 75 and 150°C with each of the three aromatic precursors. In all cases, the GPC (growth per cycle) decreased with increasing temperature. In-situ infrared spectroscopy indicated that a ring opening reactions occurred in each ABC sequence. Compositional analysis using time-of-flight elastic recoil detection indicated that fluorine could be incorporated into the film when 3-(trifluoromethyl)phenol and 2-fluoro-4-(trifluoromethyl)benzaldehyde were used as precursors.

INTRODUCTION

MLD (Molecular Layer Deposition) is fundamentally a modified ALD technique, where pinhole free, uniform nanofilms are produced with self-limiting reaction chemistry.[1] MLD can be used for manufacturing both purely organic and organic-inorganic hybrid films. The first polymer films, polyimides, deposited by the MLD technique were presented in the beginning of the 1990s [2] and since then MLD processes for a vast number of different materials, including polymers, such as polyimides, polyamides and polyureas, in addition to hybrid materials and structures such as metalcones, polymeric fibres and barrier layers have been presented.[3-7]

Compared to traditional inorganic ALD processes, MLD enables the use of numerous diverse organic compounds, thus opening up the pathway for organic thin film layers with different properties and characteristics. In MLD, properties of both organic and inorganic materials can be mixed.[8910] With organic materials, mechanical and physical properties can be greatly varied when compared to brittle ceramic materials. Because of this unprecedented tunability, novel MLD materials are continuously developed, although with certain limitations. Organic materials often possess poorer thermal stability, which restricts the maximum deposition temperatures. In addition, there is an increasing interest to modify MLD material properties by incorporating functional side chains or heteroatoms and to apply MLD coatings onto thermally sensitive substrates. For example in the case of fluorine, enhancement in optical and electronic properties can be expected.[11,12] However, additional heteroatoms, multiple functional groups or long hydrocarbon chain lengths increase precursor molecular weight, thus decreasing the vapour pressure and their usability as MLD precursors. Therefore, it is challenging to find suitable precursors with sufficient vapour pressures for low-temperature MLD processes.

One possible solution to tackle low volatility is to use monofunctional aromatic compounds, which have higher vapour pressures than heavily substituted compounds. Unfortunately, MLD growth cannot be sustained with only one functional group per precursor molecule, given that after one cycle the growth terminates due to a lack of reactive sites during the next precursor exposure. This phenomenon has been utilised in selective ALD with self-assembled monolayers (SAMs) to efficiently block film growth on certain substrate areas.[13-15] However, adsorbed monofunctional aromatic cyclic compounds can be opened and activated after they have adsorbed to the substrate, allowing continuous MLD process with consecutive cycles. In this paper, we propose a new way to enable continuous three-step processes with monofunctional aromatic precursor and ring opening reactions using phenol, 3-(trifluoromethyl)phenol, 2-fluoro-4-(trifluoromethyl)benzaldehyde together with TMA (trimethylaluminum) and O_3 (Figure 1a). Previously ozone have been used functionally in MLD processes, when Huang and his colleagues changed alkene terminal groups to carboxylic acids in the process with 7-octenytrichlorosilane, TMA and O_3.[16] In addition, ozone has been used in a MLD process to produce carbosiloxane thin films.[17] Furthermore, in conventional organic chemistry, O_3 has been exploited for oxidative cleavage of double bonds in aromatic rings leading to the opening of the aromatic ring structure and finally to the formation of carboxylic acid groups.[18-20] In our study, in the case of phenol and 3-(trifluoromethyl)phenol, a single –OH group can react with the substrate bound TMA. With 2-fluoro-4-(trifluoromethyl)benzaldehyde, the reaction happens between a Lewis acid (TMA) and nucleophilic carbonyl oxygen (Figure 1 b).[21,22] Exploiting these approaches, a new way of manufacturing novel low-temperature processes for MLD coatings is presented. In addition, incorporation of fluorine heteroatoms and the effects of hydrogen peroxide are studied.

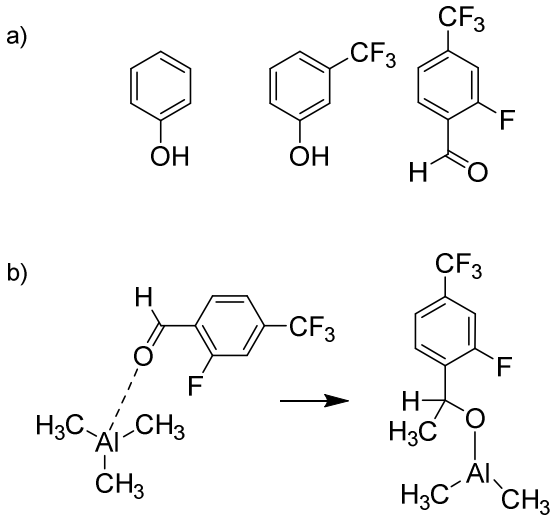

Figure 1. a) Aromatic precursors used in MLD processes. From left: phenol, 3-(trifluoromethyl)phenol (3F), 2-fluoro-4-(trifluoromethyl)benzaldehyde (4F) b) Reaction between TMA and 2-fluoro-4-(trifluoromethyl)benzaldehyde. Figure b is reconstructed from the reference [22].

EXPERIMENTAL

Deposition processes

MLD films were deposited using an ALD Picosun R-200 tool in single wafer mode. N_2 (>99.999%) from LNG (liquid nitrogen gas) was used as a carrier gas. Si (100) (Siltronic Corp.) were used as substrates throughout this study. Three- and four-step (ABC, ABCD) processes were constructed from TMA (99.999% SAFC) as a metal precursor, ozone (generated by IN USA, Inc. ozone generator from 99.99% O_2), hydrogen peroxide (50 wt.% in water, Sigma Aldrich) and aromatic precursors including phenol (> 96% Sigma-Aldrich), 3-(trifluoromethyl)phenol (99% Sigma-Aldrich) (3F) and 2-fluoro-4-

(trifluoromethyl)benzaldehyde (98% Sigma-Aldrich) (4F). A TMA precursor was stored in a metallic container and evaporated at room temperature. Phenol and 3-(trifluoromethyl)phenol were evaporated at 80°C and 2-fluoro-4-(trifluoromethyl)benzaldehyde at 60°C. Deposition temperatures varied between 75°C and 200°C.

Characterization

Thicknesses of the deposited films were measured by ex-situ ellipsometry (Sentech SE400adv). Thickness and density were also studied with XRR (X-Ray Reflectivity, Aalto University). XRR measurements were performed using an X'Pert PRO PANalytical tool with parallel beam conditions, and using Cu-Kα radiation. The acceleration voltage was 45 kV and the current was 40 mA. The incidence angle was varied from 0.3 to 3 degrees. XRR results were analysed with X'Pert Reflectivity software. Thickness was determined by fitting a simulated curve to the measured data and density by measuring the critical angle using the TOF-ERDA results. Contact angles were measured with the KSV CAM200 Optical Contact Angle Meter. Angles were measured with deionised water for testing hydrophilicity of the films. Elemental compositions were determined with TOF-ERDA (University of Jyväskylä). The beam used in TOF-ERDA analysis was 8.515 MeV $63Cu^{4+}$ and the geometry was 20.5+20.5=41 degrees.[23] The chemical structure of the films was identified after the depositions, with a Fourier transform infrared (Nicolet iS50 FTIR) spectrometer using a single-reflection 60-degree germanium attenuated total reflectance (ATR) crystal of the horizontal accessory VariGATR™. ATR-IR spectra were collected by averaging 64 scans at a resolution of 4 cm^{-1}. Measured Si chips were approximately size of 2×2 cm^2. A reproducible contact between the sample chip and the Ge ATR crystal was obtained by the built-in pressure applicator with slip-clutch of VariGATR™

accessory. In-situ FTIR (Ghent University, Belgium) depositions were made on regular Si (100) substrates, with a home-built ALD tool, which was connected to FTIR measurement equipment in transmission mode (Bruker Tensor 27, globar mid-IR source and KBr beamsplitter).

RESULTS AND DISCUSSION

Based on the ellipsometry measurements, the highest GPC of 5.4 Å/cycle was achieved by using TMA+phenol+O_3 at 80^{o}C (Specific values in supportive information, Table S1). GPC decreased with increasing deposition temperature from 80°C to 200°C (Figure 2 and 3). A similar trend was observed for the other evaluated processes; the GPC decreased for increasing substrate temperatures. The GPC of the TMA+3F+O_3 process reached 3.6 Å/cycle and with TMA+4F+O_3 the GPC got up to 4.6 Å/cycle. The typical decrease in MLD/ALD growth rate at higher temperatures is often explained by the decrease of reactive sites and precursors, decomposition of organic moieties or different orientations of the long-chain molecules.[24-27]

Hydrogen peroxide was added to obtain an ABCD-type pulsing sequence (TMA+organic molecule+O_3+H_2O_2). According to conventional chemistry, O_3 opens the aromatic ring and an additional oxidizing step is needed to obtain –OH groups (oxidation of the aldehydes to carboxylic acids).[19] However, it seems that H_2O_2 decreases the GPC, except for phenol process at temperatures from 100°C to 200°C. When hydrogen peroxide was used as a fourth precursor, the highest growth rate was approximately 80% of the value measured for the ABC process, but there was much more variation in the obtained values.

Linearity of the film growth as a function of number of MLD cycles was tested for all aromatic precursors at 100°C without hydrogen peroxide. According to the thickness results, all processes produced ALD-type films with linear growth as a function of the number of cycles (Supportive

information, Figure S1, Table S2). Furthermore, saturation was tested as a function of pulse length of the aromatic precursor. Relatively long pulse times were needed for fluorinated organic precursors, but eventually processes started to saturate (supportive information, Figures S2 and S3). The process with phenol precursor was saturated already with pulse length of 0.2 seconds (Figure 4). When the organic precursor was not used, growth rate decreased near to the growth rate of Al_2O_3. The effect of ozone on the film growth was also tested. It was discovered, that GPC increased as a function of length of O_3 pulse until stabilisation (approximately 2s, depending on the process) and finally decreased slightly in the limits of measured pulse length (5s, Figure 5). A similar trend was observed also for 3F process (supportive information, Figure S4). XRR measurements were carried out as a reference for ellipsometry data. Regardless of the measurement technique, no difference in film thickness was observed, even after several months of storage in ambient air, indicating good film stability. Quite often, hybrid MLD films have been observed to be unstable against moisture due to the unreacted precursors or weak M-R or M-O-R bonds.[7,28]

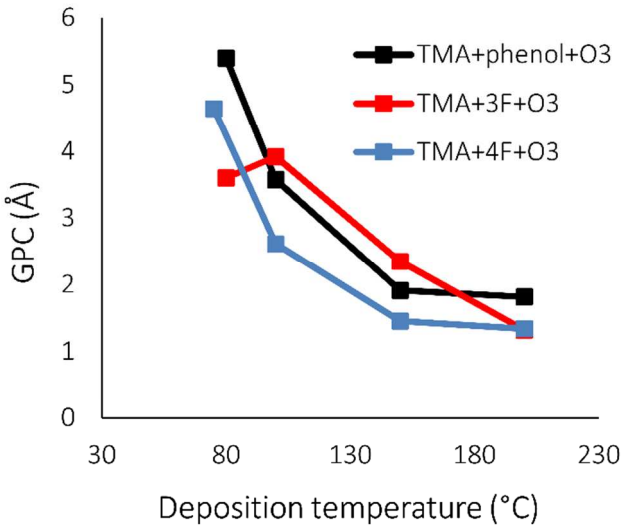

Figure 2. GPC of ABC processes as a function of deposition temperature. The thicknesses were measured after 200 cycles.

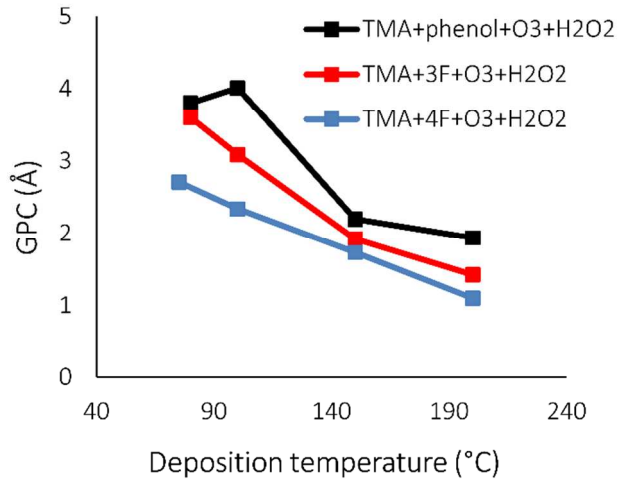

Figure 3 GPC of ABCD processes as a function of deposition temperature. The thicknesses were measured after 200 cycles

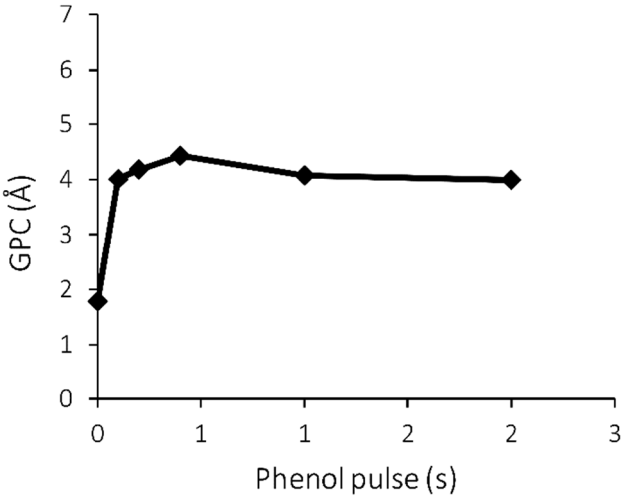

Figure 4. GPC as a function of the phenol pulse length. Films were deposited at 100°C.

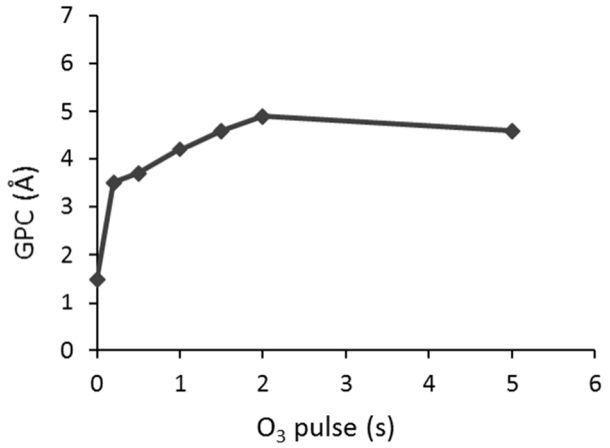

Figure 5. GPC as a function of the O_3 pulse length. Process with TMA, phenol and O_3. Films were deposited at 100°C.

Contact angles were determined with deionised water for testing the hydrophilicity of the films deposited at 100°C (Table 1). In all processes, the terminal MLD step was ozone or hydrogen peroxide, depending on the process. Aluminium oxide (Al_2O_3) was manufactured from TMA and O_3 as reference material. Films deposited with 4F had the highest contact angles, 73° and 74° (with H_2O_2). Furthermore, these angles corresponded to the utmost with the Al_2O_3 reference material (70°). Films deposited with 3F had notably smaller contact angles of 58° and 51° (with H_2O_2). Contact angles for the films with phenol were 60° and 58° (H_2O_2).

Table 1. Contact angles with deionised water for MLD films deposited on Si at 100°C.

Process	Contact angle (°)
TMA+O_3	70

TMA+phenol+O_3	60
TMA+phenol+O_3+H_2O_2	58
TMA+3F*+O_3	58
TMA+3F +O_3+H_2O_2	51
TMA+4F**+O_3	73
TMA+4F+O_3+H_2O_2	74

*3F: 3-(trifluoromethyl)phenol

**4F: 2-fluoro-4-(trifluoromethyl)benzaldehyde

The process based on 4F had the highest contact angles and angles closest to Al_2O_3. Similarity between the 4F process and pure Al_2O_3 is probably due to the fact that films produced with 4F exhibited the highest relative aluminium and oxygen content and a relatively low amount of the hydrocarbons. In the case of TMA+4F+O_3, a reaction happens between carbonyl oxygen and aluminium, and coverage stays smaller, whereas in the case of phenol and 3F, the reaction occurs between a hydroxyl group and TMA, and the coverage grows bigger due to the more favourable reaction. Furthermore, the coverage of 4F is probably smaller because of the bigger molecular size resulting in steric hindrance. Differences in coverage are directly proportional to the amount of organic structures and free carboxylic acids. It is also likely that the amount of incorporated fluorine atoms affect the hydrophilicity, which explains the difference of contact angles between phenol and 3F processes. Films deposited with 3F had the smallest contact angles (58° and 51°), i.e., the biggest hydrophilicity. The use of hydrogen peroxide caused the decrease of the angles in the cases of phenol and 3F. This is likely due to the increasing amount of carboxylic acids, produced by hydrogen peroxide. Hydrogen peroxide had no clear effect on the process with 2-fluoro-4-(trifluoromethyl)benzaldehyde.

TOF-ERDA measurements were performed for the films deposited by TMA+4F+O_3 at 75°C and by TMA+phenol+O_3 and TMA+3F+O_3 at 100°C (For TOF-energy histograms and depth profiles, see supportive information, Figures S5-S16). The oxygen content was the highest in the case of TMA+4F+O_3 and the lowest in the films deposited from TMA+3F+O_3, whereas carbon content had a just opposite trend. According to the TOF-ERDA results, the Al:O ratio in the films is lower (0.4), than the Al:O ratio in pure Al_2O_3 suggests (0.7) (Table 3). This can be explained with the carboxylic acid formation during O_3 pulse and the ring opening reaction. It is probable that a subsequent TMA pulse reacts with carboxyl groups forming bidentate and bridging complexes, resulting in an excess of oxygen in every cycle. Ratios of aluminium and carbon vary between 0.7 and 1.6.

Table 2. TOF-ERDA measurements of the elemental compositions (at-%) of all processes.

Sample	Al	O	H	C	N	F
TMA+phenol+O_3	13±2	41±3	30±3	15±2	0.3±0.1	0
TMA+phenol+O_3+H_2O_2	15±1	38±2	31±3	15±1	0.2±0.1	0
TMA+3F*+O_3	13±2	37±3	27±3	16±2	0.3±0.1	8±1
TMA+3F+O_3+H_2O_2	13±2	36±3	25±3	18±2	0.6±0.2	7.4±1.0
TMA+4F**+O_3	16±2	45±4	26±3	10±1	0.7±0.2	1.9±0.5
TMA+4F+O_3+H_2O_2	17±3	42±4	26±3	11±3	0.8±0.3	2.9±0.6

*3F: 3-(trifluoromethyl)phenol

**4F: 2-fluoro-4-(trifluoromethyl)benzaldehyde

Fluorine incorporation was obtained with both processes based on 3F and 4F compounds. When using 3F as an organic precursor, 8% and 7.4% of fluorine was detected in the films from

TMA+3F+O_3 and TMA+3F+O_3+H_2O_2 processes, respectively. Similarly, 4F processes, with and without H_2O_2, resulted in 1.9% and 2.9% of fluorine, respectively. According to the TOF-ERDA results, more fluorine was incorporated into the films when using 3F, which has less fluorine atoms in its molecule compared to the 4F (Figure 1a). It is unlikely, that the ozone would not affect on the double bonds still remaining in the structure after the ring-opening reaction. It is possible, that after aromatic ring opening, the subsequent ozone pulse breaks a second double bond from the carbon chain, thus forming a new carboxylic acid structure and decreasing the amount of carbon of the original aromatic ring. Differences between processes can be explained with the cleavages of different double bonds in aromatic structures (Figure 6). It is expected, that in the case of 3F, the majority of the cleavages focus on the C3-C4 double bond, whereas in the case of 4F, the majority focus on the C1-C2 double bond, thus diminishing the amount of fluorine atoms substantially. The trends for Al and C compositions in the TOF-ERDA data can be understood based on these considerations. Furthermore, the relative amounts of fluorine are explained with these second cleavages induced by ozone. It is also probable, as indicated by the lower deposition rate, that the surface coverage of the bulky 4F might not be as high as it is in the case of other organic precursors, hence the bigger Al:C ratio in the TOF-ERDA results. However, as there are several possibilities for reactions during the second O_3 pulse and following the TMA pulse, more detailed research via modelling is needed.

Table 3. Ratios between elements according to the TOF-ERDA measurements.

Sample	Al:O	Al:C	C:H	F:C
TMA+phenol+O_3	0.3	0.9	0.5	0
TMA+phenol+O_3+H_2O_2	0.4	1.0	0.5	0

TMA+3F+O_3	0.4	0.8	0.6	0.5
TMA+3F+O_3+H_2O_2	0.4	0.7	0.7	0.4
TMA+4F+O_3	0.4	1.6	0.4	0.2
TMA+4F+O_3+H_2O_2	0.4	1.6	0.4	0.3

Densities measured by XRR were 2.1 - 2.4 (g/cm^3) for the films deposited by three different processes (Table 4). Films deposited by the TMA+4F+O_3 process had the highest density, 2.4 g/cm^3, which is explained with the lowest content of the organic compounds, compared to other processes, hence the highest ratio between aluminium and carbon.

Table 4. XRR measurements of film thicknesses and calculated densities (g/cm^3). Deposition temperature 100°C, 200 cycles.

Sample	GPC (Å)	Density g/cm^3
TMA+phenol+O_3	3.9	2.1
TMA+phenol+O_3+H_2O_2	3.5	2.2
TMA+3F+O_3	4.3	2.1
TMA+3F+O_3+H_2O_2	3.3	2.2
TMA+4F+O_3	2.4	2.4
TMA+4F+O_3+H_2O_2	2.8	2.4

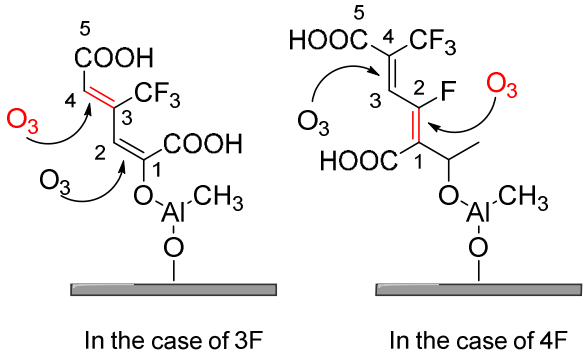

Figure 6. Possible bond cleavages during the second ozone pulse. In the case of 3F, the majority of the cleavages focus on the C3-C4 double bond, whereas in the case of 4F, the majority focusses on the C1-C2 double bond.

ATR-IR spectra for all processes are presented in Figures 7-9. Hydroxyl groups of carboxylic acid (3100-3600 cm^{-1}), CO_2^- and CO_2-Al structures (1389-1397 cm^{-1}, 1606-1616 cm^{-1} and 1420-1390 cm^{-1}), and Al-O stretches (704-879 cm^{-1}) were observed regardless of the process used (Table 5). In addition, the carbonyl group band (1720 cm^{-1}) of carboxylic acid can be seen as a shoulder in all three spectra. The incorporation of a fluorinated aromatic precursor was evidenced by the strong band of C-F structure for films deposited by the TMA+3F+O_3 process seen at 1123 cm^{-1} and 1124 cm^{-1}. Furthermore, in films deposited by the TMA+3F+O_3 and TMA+4F+O_3 processes, a band around 1320-1340 cm^{-1} (CF_3 attached to benzene ring) was observed. These bands are missing in the spectra of non-fluorinated phenol derived films. When phenol or 3F was used as the organic precursor in the ABCD-type reaction, H_2O_2 did not induce significant changes to the ATR-IR spectra obtained. In the case of 4F with H_2O_2, there is an additional band at 1336 cm^{-1}, probably originating from the stretch of CF_3 attached to a benzene ring.

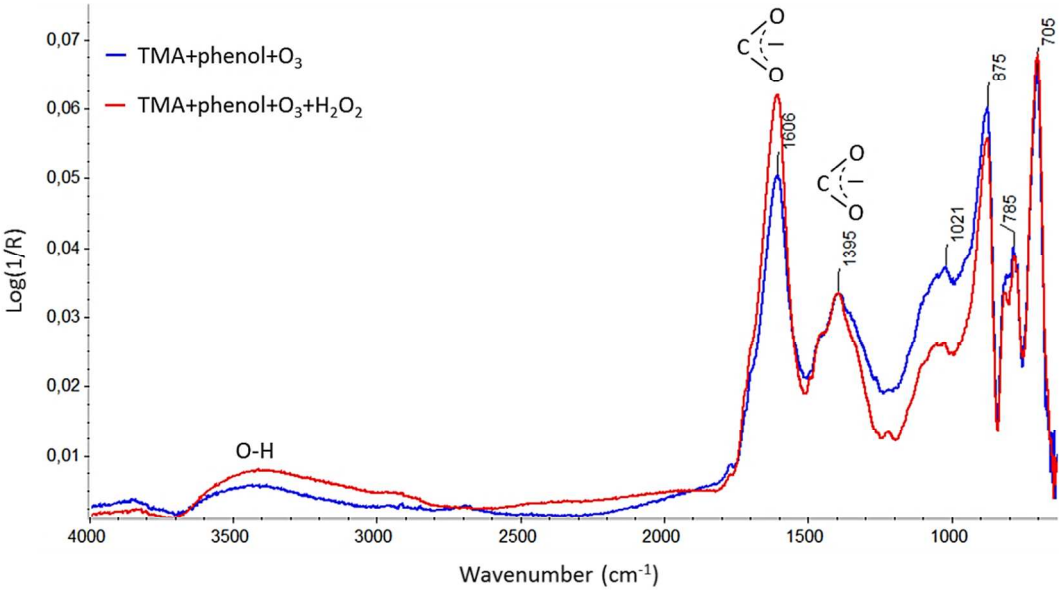

Figure 7. ATR-FTIR spectra of 72 nm and 80 nm thick films deposited by TMA+phenol+O_3 and TMA+phenol+O_3+H_2O_2 processes, respectively. Films deposited at 100°C.

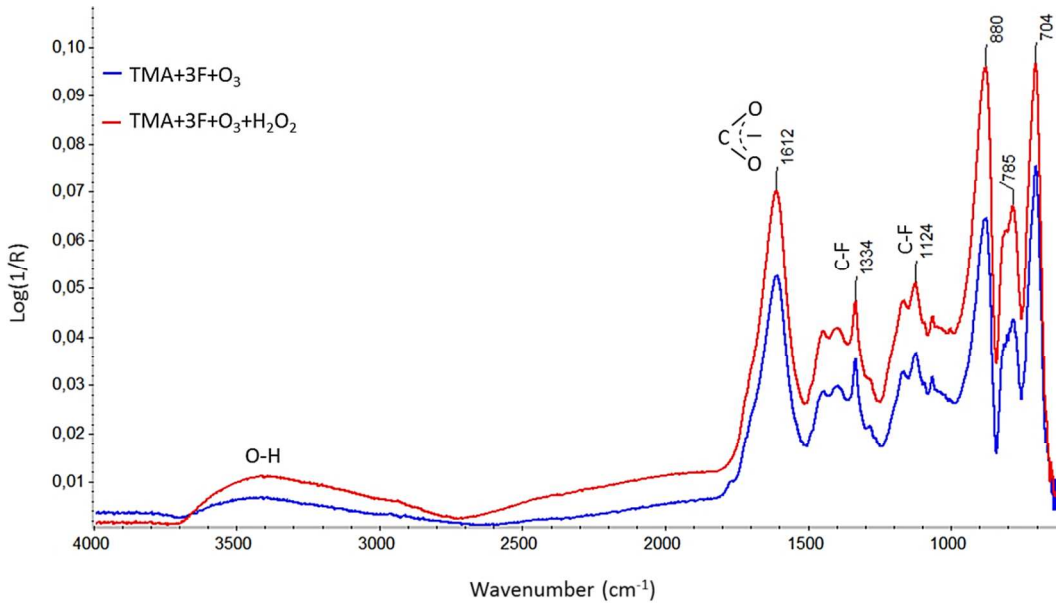

Figure 8. ATR-FTIR spectra of 78 nm and 62 nm thick films deposited by TMA+3-(trifluoromethyl)phenol+O_3 and TMA+3-(trifluoromethyl)phenol+O_3+H_2O_2 –processes, respectively. Films deposited at 100°C.

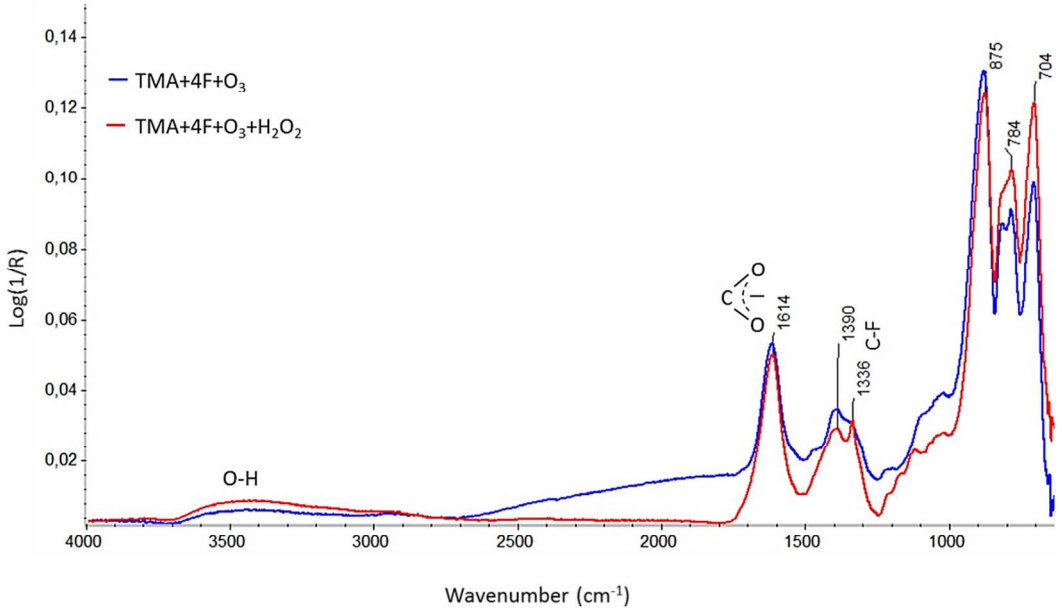

Figure 9. ATR-FTIR spectra of 93 nm and 54 nm thick films deposited by TMA+2-(fluoro-4-(trifluoromethyl)benzaldehyde+O_3 and TMA+2-fluoro-4-(trifluoromethyl)benzaldehyde+O_3+H_2O_2 processes, respectively. Films deposited at 75°C.

Table 5. ATR-IR band assignments for deposited MLD films. Processes with H_2O_2 are included.[29–31]

Process	Frequency (cm^{-1})	Assignment
TMA+ phenol+O_3	3100-3600	O-H stretching
	1720	C=O carboxylic acid stretching
	1606	COO^- antisymmetric stretching
	1395	COO^- symmetric stretching
	705-875, 1021	Al-O
TMA+3F+O_3	3100-3600	O-H stretching
	1720	C=O carboxylic acid stretching
	1611,1612	COO^- antisymmetric stretching
	1397	COO^-symmetric stretching
	1334	CF_3 attached to benzene ring
	1123,1124	Aliphatic CF_3, C-F in aliphatic fluoro compounds
	704-879, 1065	Al-O
TMA+4F+O_3	3100-3600	O-H stretching
	1720	C=O carboxylic acid stretching
	1616	COO^- antisymmetric stretching
	1389	COO^-symmetric stretching
	1320-1340	CF_3 attached to benzene ring
	704-879	Al-O

In-situ transmission FTIR spectra were collected during 200 deposition cycles and the sum of the differential spectra were averaged out from all the events. Examples of in-situ FTIR spectra are presented in Figures 10 and 11. According to these results, it seems evident that the ring opening reaction is occurring between aromatic precursors and O_3. In the TMA spectra, there is a clear stretching vibration band from deformation of Al-CH_3 (1205 cm^{-1}) and antisymmetric CH_3 stretching band (2936 cm^{-1}).[31] After an aromatic precursor pulse, there is a negative absorbance in the area of CH_3 stretching (2936 cm^{-1}), when the CH_3 structures disappear. Furthermore, after the aromatic precursor pulse, the absorption bands at 1495 cm^{-1}, 1595 cm^{-1} and 3030-3070 cm^{-1} can be seen and attributed to the aromatic structure.[32] With 3F and 4F pulses, also bands originating from the CF_3 stretch at 1328 cm^{-1} and 1330 cm^{-1}, as well as the C-F stretch at 1000-1200 cm^{-1} can be distinguished.[30,32] In the case of phenol, aromatic C-O stretching band is observed (1295 cm^{-1}).[29] The subsequent third precursor, the O_3 pulse, removes aromatic species as evidenced by the negative absorbance (1495 cm^{-1}, 3020-3070 cm^{-1}) in the difference spectra near the aromatic band regions. At the same time carbonyl group (C=O) stretching vibration from carboxylic acid and carboxylate ion (CO_2^-) bands appear at 1726 cm^{-1}, 1610 cm^{-1} and 1465-1590 cm^{-1} (Figure 11).[33-35] The O_3 pulse affects the fluorine bonding as well, since band originating from the CF_3 structure attached to benzene ring is substituted with band of aliphatic C-F at 1200-1300 cm^{-1}, as detected in processes with 3F or 4F. In addition, after O_3 pulse observed hydroxyl band above 3200 cm^{-1} is originating from carboxyl acids further supporting the ring opening theory. As expected, the bands originating from –OH groups disappear during the subsequent TMA pulse and the reaction forms the CO_2-Al structure. The obtained band frequencies from in-situ FTIR (Table 6) and ex-situ ATR-IR correspond well to each other, indicating similarity of the ALD-processes despite the different equipment. Although, it is good

to mention, that the reactions in the films analysed by ATR-IR where not as completed as during the in-situ FTIR, since there were still some aromatic structures left in the deposited films used in the ATR-IR analysis in the case of 3F and 4F (CF_3 structure attached to benzene ring, 1320-1340 cm^{-1}). To be able to make further conclusions about the role of H_2O_2, more detailed research with in-situ FTIR is needed.

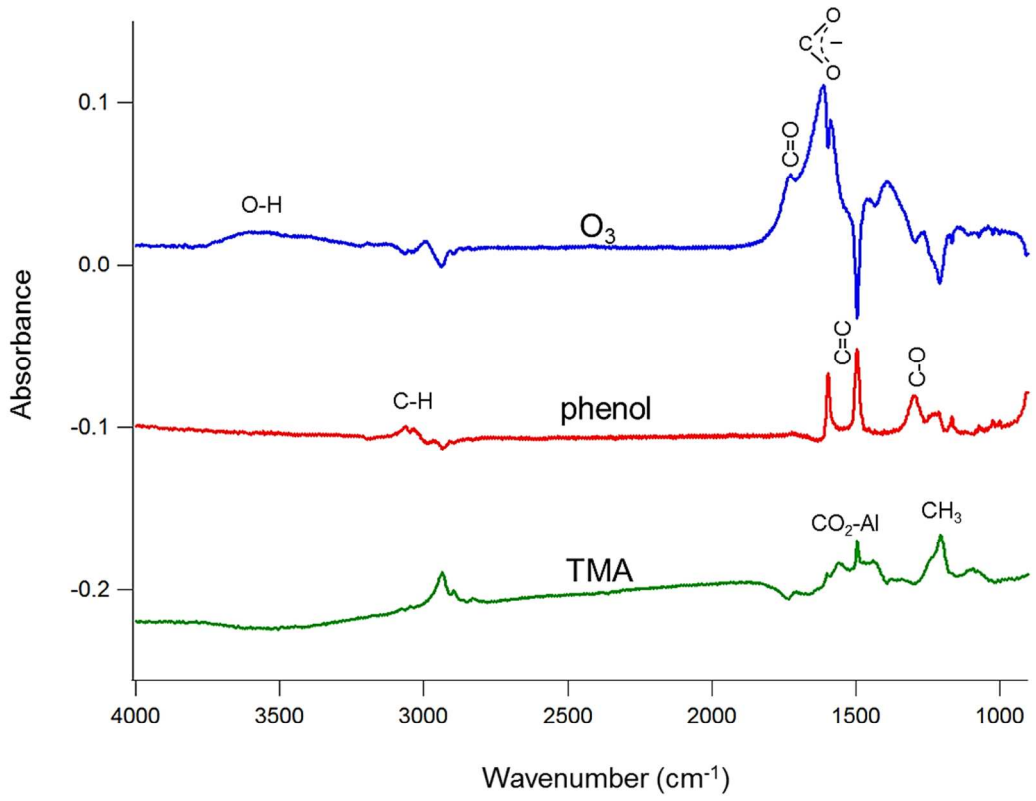

Figure 10. In-situ FTIR averaged out difference spectra after 200 cycles of TMA+phenol+O_3 pulses at 100°C onto Si-wafer.

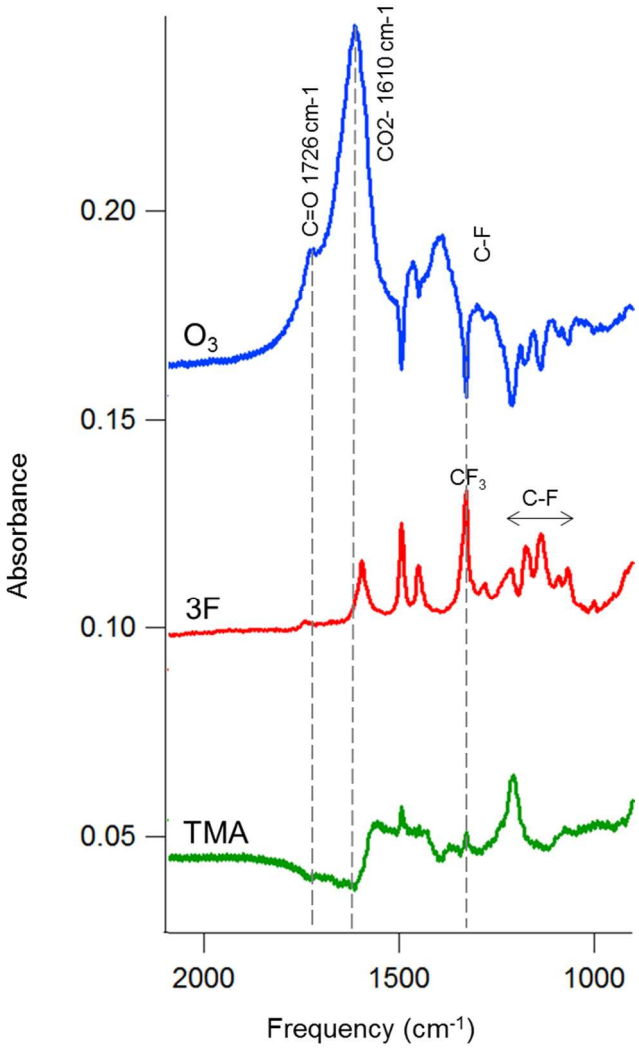

Figure 11. In-situ FTIR averaged out difference spectra after 200 cycles of TMA+3-(trifluoromethyl)phenol+O_3 pulses at 100°C onto Si-wafer.

Table 6. In-situ FTIR band assignments for processes with TMA + phenol /3F /4F + O_3. Temperature in all processes 100°C, 200 cycles.[29-35]

Precursor pulse	Observed frequency (cm^{-1})	Assignment
TMA	2936	CH_3 antisymmetric stretching / C-H stretching
	1560	COO- bidentate antisym. stretching
	1495	COO- bidentate sym. stretching
	1205	Al-CH_3 sym. deformation
	< 1000	Al-O
Phenol	3030-3070	Aromatic C-H stretching
	1595	Aromatic C=C stretching
	1495	
	1295	Aromatic C-O stretching
3-(trifluoromethyl)-phenol	3030-3070	Aromatic C-H stretching
	1595	Aromatic C=C stretching
	1495	
	1450	Antisymmetric CH_3 deformation
	1328	CF_3 attached to benzene ring
	1280	Aromatic C-O
	1050-1200	C-F
4-fluoro-3-(trifluoromethyl)-benzaldehyde	3060	Aromatic C-H stretching
	1595	Aromatic C=C stretching
	1495	

	1450	Antisym. CH_3 deformation
	1330	CF_3 attached to benzene ring
	1000-1200	C-F
Ozone	3200-3765	O-H stretching
	1726	C=O carboxylic acid
	1610	OCO antisym. stretchings
	1590	
	1465	OCO symmetric stretch, in the cases of 3F ja 4F
	1200-1300	C-F stretch in aliphatic fluoro compounds in case of 3-(trifluoromethyl) phenol and 2-fluoro-4-(trifluoromethyl) benzaldehyde

Both in-situ FTIR and TOF-ERDA measurements support the ring opening reaction during MLD deposition. Based on the presented results, the following reactions during one cycle in the process with TMA + phenol + O_3 can be suggested (Figure 12).

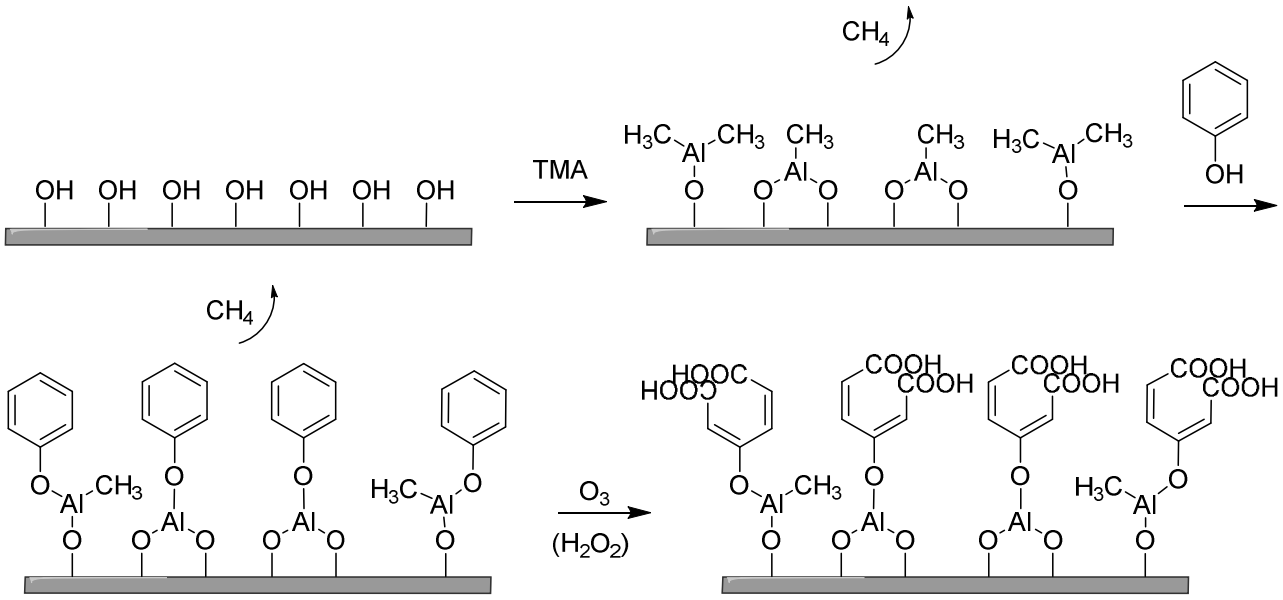

Figure 12. Suggested reactions during one cycle in the TMA+phenol+O_3(+H_2O_2) process.

CONCLUSIONS

The monofunctional aromatic precursors used in this study can be applied for the MLD processes, and self-limiting growth can be obtained. Depending on the aromatic precursor, depositions can be performed at temperatures even as low as 75-100°C, thus opening up new possibilities for coating temperature-sensitive substrates by MLD materials. According to the ATR-IR, in-situ FTIR and TOF-ERDA measurements, it can be confirmed that fluorine was incorporated into the deposited films and ring opening reaction occurred between aromatic compounds and O_3. Elucidating the role of H_2O_2 will require further efforts by in-situ FTIR, QCM and modelling.

AUTHOR INFORMATION

Corresponding Author

*Email: laura.svard@vtt.fi

Author Contributions

The manuscript was written through contributions of all authors. All authors have given approval to the final version of the manuscript.

Funding Sources

This research was supported by the Academy of Finland (project ID 288212).

Notes

The authors declare no competing financial interest.

ACKNOWLEDGEMENTS

This research was supported by the Academy of Finland (project ID 288212 and 251353).

ASSOCIATED CONTENT

Supporting information. More detailed information of GPC, linearity as a function of number of cycles, saturation, effect of ozone and TOF-ERDA.

REFERENCES

(1) Ritala, M.; Leskelä, M.; Dekker, J.-P.; Mutsaers, C.; Soininen, P. J.; Skarp, J. Perfectly Conformal TiN and Al2O3 Films Deposited by Atomic Layer Deposition**. *Chem. Vap. Depos.* **1999**, *5* (1), 7–9.

(2) Yoshimura, T.; Tatsuura, S.; Sotoyama, W. Polymer Films Formed with Monolayer Growth Steps by Molecular Layer Deposition. *Appl. Phys. Lett.* **1991**, *59* (4), 482–484.

(3) Hirvikorpi, T.; Vähä-nissi, M.; Mustonen, T.; Iiskola, E.; Karppinen, M. Atomic Layer Deposited Aluminum Oxide Barrier Coatings for Packaging Materials. *Thin Solid Films* **2010**, *518* (10), 2654–2658.

(4) George, S. M. Hybrid Organic-Inorganic Films Grown Using Molecular Layer Deposition. **2011**, 12–26.

(5) Gregorczyk, K.; Knez, M. Hybrid Nanomaterials through Molecular and Atomic Layer Deposition: Top Down, Bottom Up, and in-between Approaches to New Materials. *Prog. Mater. Sci.* **2016**, *75*, 1–37.

(6) Lee, B. H.; Yoon, B.; Abdulagatov, A. I.; Hall, R. A.; George, S. M. Growth and Properties of Hybrid Organic-Inorganic Metalcone Films Using Molecular Layer Deposition Techniques. *Adv. Funct. Mater.* **2013**, *23* (5), 532–546.

(7) Dameron, A. A.; Seghete, D.; Burton, B. B.; Davidson, S. D.; Cavanagh, A. S.; Bertrand, J. A.; George, S. M. Molecular Layer Deposition of Alucone Polymer Films Using Trimethylaluminum and Ethylene Glycol. *Chem. Mater.* **2008**, *20* (9), 3315–3326.

(8) Gong, B.; Peng, Q.; Parsons, G. N. Conformal Organic-Inorganic Hybrid Network Polymer Thin Films by Molecular Layer Deposition Using Trimethylaluminum and Glycidol. *J. Phys. Chem. B* **2011**, *115* (19), 5930–5938.

(9) Yoon, B.; Patchen, J. L. O.; Seghete, D.; Cavanagh, A. S.; George, S. M. Molecular Layer Deposition of Hybrid Organic-Inorganic Polymer Films Using Diethylzinc and Ethylene Glycol **. *Chem. Vap. Depos.* **2009**, *15*, 112–121.

(10) Klepper, K. B.; Nilsen, O.; Fjellvag, H. Deposition of Thin Films of Organic-inorganic Hybrid Materials Based on Aromatic Carboxylic Acids by Atomic Layer Deposition. *Dalt. Trans.* **2010**, *39* (48), 11628–11635.

(11) Francesco Babudri, Gianluca M. Farinola, Francesco Naso, R. R. Fluorinated Organic Materials for Electronic and Optoelectronic Applications. The Role of the Fluorine Atom.pdf. *Chem. Commun.* **2007**, 1003–1022.

(12) Chini, M. K.; Chatterjee, S. Effect of Side-Chain Functionality on the Organic Field-Effect Transistor Performance of Oligo (P -Phenylenevinylene) Derivatives. **2017**, *134* (22), 44825.

(13) Kim, W.-H.; Lee, H.-B.-R.; Heo, K.; Lee, Y. K.; Chung, T.-M.; Kim, C. G.; Hong, S.; Heo, J.; Kim, H. Atomic Layer Deposition of Ni Thin Films and Application to Area-Selective Deposition. *J. Electrochem. Soc.* **2011**, *158* (1), D1–D5.

(14) Chen, R.; Bent, S. F. Chemistry for Positive Pattern Transfer Using Area-Selective Atomic Layer Deposition. *Adv. Mater.* **2006**, *18* (8), 1086–1090.

(15) Prasittichai, C.; Zhou, H.; Bent, S. F. Area Selective Molecular Layer Deposition of Polyurea Films. *Appl. Mater. Interfaces* **2013**, *5*, 13391–13396.

(16) Huang, B. J.; Lee, M.; Lucero, A.; Kim, J. Organic-Inorganic Hybrid Nano-Laminates Fabricated by Ozone-Assisted Molecular-Atomic Layer Deposition **. *Chem. Vap. Depos.* **2013**, *19* (4-6), 142–148.

(17) Zhou, H.; Bent, S. F. Highly Stable Ultrathin Carbosiloxane Films by Molecular Layer Deposition. *J. Phys. Chem. C* **2013**, *117* (39), 19967−19973.

(18) Bailey, P. S. The Reactions of Ozone with Organic Compounds. *Chem. Rev.* **1958**, *58* (5), 925–1010.

(19) Shen, Y.; Lei, L.; Zhang, X.; Zhou, M.; Zhang, Y. Effect of Various Gases and Chemical Catalysts on Phenol Degradation Pathways by Pulsed Electrical Discharges. *J. Hazard. Mater.* **2008**, *150* (3), 713–722.

(20) Youmin, S.; Xiaohua, R.; Zhaojie, C. The Degradation Mechanism of Phenol Induced by Ozone in Wastes System. *J. Mol. Model.* **2012**, *18*, 3821–3830.

(21) Smith, J. D. Aluminium: Annual Survey Covering the Year 1975. *J. Organomet. Chem.* **1977**, *130*, 303.

(22) Gong, B.; Parsons, G. N. Caprolactone Ring-Opening Molecular Layer Deposition of Organic-Aluminum Oxide Polymer Films. *ECS J. Solid State Sci. Technol.* **2012**, *1* (4), P210–P215.

(23) Laitinen, M.; Rossi, M.; Julin, J.; Sajavaara, T. Time-of-Flight - Energy Spectrometer for Elemental Depth Profiling - Jyv??skyl?? Design. *Nucl. Instruments Methods Phys. Res.*

Sect. B Beam Interact. with Mater. Atoms **2014**, *337*, 55–61.

(24) Dillon, A. C.; Ott, A. W.; Way, J. D.; George, S. M. Surface Chemistry of Al , O , Deposition Using Al (CH ,) 3 and H , O in a Binary Reaction Sequence. *Surf. Sci.* **1995**, *322* (1-3), 230–242.

(25) Puurunen, R. L.; Lindblad, M.; Krause, A. O. I.; Hut, F. I. N.; Oil, F.; Oy, G.; Box, P. O.; Um, F. I. N. F.; Oil, F.; Oy, G.; et al. Successive Reactions of Gaseous Trimethylaluminium and Ammonia on Porous Alumina. *Phys. Chem. Chem. Phys.* **2001**, *3* (6), 1093–1102.

(26) Puurunen, R. L. Surface Chemistry of Atomic Layer Deposition: A Case Study for the Trimethylaluminum/water Process. *J. Appl. Phys.* **2005**, *97* (12), 121301–1213053.

(27) Sundberg, P.; Karppinen, M. Organic and Inorganic-Organic Thin Film Structures by Molecular Layer Deposition: A Review. *Beilstein J. Nanotechnol.* **2014**, *5* (1), 1104–1136.

(28) Peng, Q.; Gong, B.; Vangundy, R. M.; Parsons, G. N.; Carolina, N. " Zincone " Zinc Oxide - Organic Hybrid Polymer Thin Films Formed by Molecular Layer Deposition. *Chem. Mater.* **2009**, *21* (10), 820–830.

(29) Choudhury, D.; Sarkar, S. K. Molecular Layer Deposition of Alucone Films Using Trimethylaluminum and Hydroquinone. *J. Vac. Sci. Technol. A Vacuum, Surfaces, Film.* **2015**, *33* (1), 1–8.

(30) Ernö Pretsch, P. B.; Badertscher, M. *Structure Determination of Organic Compounds*; 2009.

(31) Yoon, B.; Seghete, D.; Cavanagh, A. S.; George, S. M. Molecular Layer Deposition of Hybrid Organic - Inorganic Alucone Polymer Films Using a Three-Step Abc Reaction Sequence. *Chem. Mater.* **2009**, *21* (22), 5365–5374.

(32) Lambert, J. B. *Introduction to Organic Spectroscopy*; MacMillan: New York, 1987.

(33) Klepper, K. B.; Nilsen, O.; Francis, S.; Fjellvåg, H. Guidance of Growth Mode and Structural Character in Organic-Inorganic Hybrid Materials - a Comparative Study. *Dalton Trans.* **2014**, *43* (9), 3492–3500.

(34) Goldstein, D. N.; McCormick, J. a.; George, S. M. Al2O3 Atomic Layer Deposition with Trimethylaluminum and Ozone Studied by in Situ Transmission FTIR Spectroscopy and Quadrupole Mass Spectrometry. *J. Phys. Chem. C* **2008**, *112* (49), 19530–19539.

(35) Stuart, B. *Infrared Spectroscopy: Fundamentals and Applications*, 1st ed.; John Wiley and sons: GB, 2004.

Graphic for Table of Contents Only